HHS Public Access

Author manuscript

*Mitochondrion*. Author manuscript; available in PMC 2017 January 01.

Published in final edited form as:

*Mitochondrion*. 2016 January ; 26: 19–25. doi:10.1016/j.mito.2015.11.001.

# Mitochondrial response in a toddler-aged swine model following diffuse non-impact traumatic brain injury

**Todd J. Kilbaugh**[a], **Michael Karlsson**[b], **Ann-Christine Duhaime**[d], **Magnus J. Hansson**[b], **Eskil Elmer**[b], and **Susan S. Margulies**[c]

[a]Department of Anesthesiology and Critical Care Medicine, Children's Hospital of Philadelphia, Perelman School of Medicine at the University of Pennsylvania, 3401 Civic Center Blvd., Philadelphia, Pennsylvania 19104, USA

[b]Mitochondrial Medicine, Department of Clinical Sciences, Lund University, BMC A13, SE-221 84 Lund, Sweden

[c]Department of Bioengineering, University of Pennsylvania, 210 South 33rd Street, Philadelphia, PA 19104, USA

[d]Department of Neurosurgery, Massachusetts General Hospital, Harvard Medical School, 15 Parkman Street, Boston, MA 02114, USA

## Abstract

Traumatic brain injury (TBI) is an important health problem, and a leading cause of death in children worldwide. Mitochondrial dysfunction is a critical component of the secondary TBI cascades. The response of mitochondria in the pediatric brain to injury has limited investigation, despite evidence that developing brain's response differs from the adult, especially in diffuse non-impact TBI. We perform a detailed evaluation of mitochondrial bioenergetics using high-

Corresponding author: Todd Kilbaugh: Department of Anesthesiology and Critical Care Medicine, The Children's Hospital of Philadelphia 34th & Civic Center Blvd, Philadelphia, PA 19104, USA, P: 267-426-7131, F: 215-590-4327, kilbaugh@chop.edu.

**Author's contact information:**

Todd Kilbaugh: Department of Anesthesiology and Critical Care Medicine, The Children's Hospital of Philadelphia 34th & Civic Center Blvd, Philadelphia, PA 19104, USA, P: 267-426-7131, F: 215-590-4327, kilbaugh@chop.edu

Michael Karlsson: Mitochondrial Medicine, Department of Clinical Sciences, Lund University, BMC A13, SE-22184 Lund, Sweden, P: +46-46-2220605, F: +46-46-2220615, michael.karlsson@med.lu.se

Ann-Christine Duhaime: 15 Parkman Street, Boston, MA 02114-3117, USA, P: 617-643-9175, F: 617-724-1866, aduhaime@partners.org

Magnus J. Hansson: Mitochondrial Medicine, Department of Clinical Sciences, Lund University, BMC A13, SE-22184 Lund, Sweden, P: +46-46-2220605, F: +46-46-2220615, magnus.hansson@med.lu.se

Eskil Elmer: Mitochondrial Medicine, Department of Clinical Sciences, Lund University, BMC A13, SE-22184 Lund, Sweden, P: +46-46-2220605, F: +46-46-2220615, eskil.elmer@med.lu.se

Susan S. Margulies: 240 Skirkanich Hall, 210 South 33rd Street, Philadelphia, PA 19104-6321, USA, 215-898-0882, FAX 215 573-2071, margulie@seas.upenn.edu

**Animal Experimentation**

All procedures were approved by the Institutional Animal Care and Use Committee of the University of Pennsylvania.

**Authors Disclosure Statement**

Eskil Elmer and Magnus J. Hansson own shares in and have received salary support from NeuroVive Pharmaceutical AB, a public company active in the field of mitochondrial medicine. Michael Karlsson has received salary support from NeuroVive Pharmaceutical AB. All other authors have no competing financial interests.

resolution respirometry in a swine model of diffuse TBI (rapid non-impact rotational injury: RNR), and examined the cortex and hippocampus. A substrate-uncoupler-inhibitor-titration protocol examined the role of the individual complexes as well as the uncoupled maximal respiration. Respiration per mg of tissue was also related to citrate synthase activity (CS) as an attempt to control for variability in mitochondrial content following injury. Diffuse RNR stimulated increased complex II-driven respiration relative to mitochondrial content in the hippocampus compared to shams. LEAK (State $4_O$) respiration was increased in both hippocampal and cortical tissue, with decreased respiratory ratios of convergent oxidative phosphorylation through complex I and II, compared to sham animals, indicating uncoupling of oxidative phosphorylation at 24 hours. The study suggests that proportionately, complex I contribution to convergent mitochondrial respiration was reduced in the hippocampus after RNR, with a simultaneous increase in complex-II driven respiration. In addition, mitochondrial respiration 24 hours after diffuse TBI that varies by location within the brain. Finally, we conclude that significant uncoupling of oxidative phosphorylation and alterations in convergent respiration through complex I- and complex II-driven respiration reveals therapeutic opportunities for the injured at-risk pediatric brain.

### Keywords

Pediatric Brain Injury; Traumatic Brain Injury; Mitochondria; In Vivo Studies; Large Animal Model of Injury

## Introduction

Traumatic brain injury (TBI) is an important health problem and is set to become the third leading cause of death and disability in the world by 2020 (Coronado et al., 2011; Gean and Fischbein, 2010).

Diffuse TBI triggers a heterogeneous insult to the brain induced by traumatic biomechanical shearing forces when the head is rapidly accelerated and/or decelerated, such as during player-to-player contacts in sports settings, impacts after falls, or whiplash injuries in car crashes. Axonal shear stretch leads to the opening of voltage-gated calcium channels that, ultimately, precipitates mitochondrial dysfunction, bioenergetic failure, and the release of secondary messengers that end in apoptosis and death (Balan et al., 2013; Glenn et al., 2003; Lifshitz et al., 2003; Marcoux et al., 2008; Ragan et al., 2013; Xu et al., 2010). Thus, mitochondria play a central role in cerebral metabolism and regulation of oxidative stress, excitotoxicity, and apoptosis in acute brain injury; however, the mechanistic response and time course following diffuse TBI, especially in the immature brain at differing developmental stages, has limit investigation (Balan et al., 2013; Gilmer et al., 2010; Lifshitz et al., 2004; Robertson et al., 2009). Furthermore, the challenge of extrapolating adult models of diffuse TBI to pediatric models includes developmental differences in biomechanical properties and biological responses that vary in the infant, toddler, adolescent, and adult (Grate et al., 2003; Ibrahim et al., 2010; S. Sullivan et al., 2015; Weeks et al., 2014). In addition, there are critical differences in mitochondrial characteristics in the developing brain as it matures, such as the number and density of complexes of the electron

transfer chain, antioxidant enzyme activity and content, and lipid content (Bates et al., 1994; Del Maestro and McDonald, 1987). Taken together, the immature brain's response to TBI changes during development from infancy through adolescence and differs with injury mechanism (Armstead, 2005; Duhaime, 2006; Duhaime et al., 2000; Durham and Duhaime, 2007). These unique features of the developing brain underscore the importance of characterizing the bioenergetic failure and cell death cascades following TBI in the immature brain in order to develop age-specific mitochondrial-directed neuroprotective approaches.

Previously we reported differences in the regional mitochondrial responses in neonatal piglets, age 3–5 days, following diffuse white matter injury using our large animal model (Kilbaugh et al., 2011). In our current investigation, we have expanded our investigation to the 4-week old animals with comparable neurodevelopment to a human toddler. Furthermore, we expanded our previous techniques to investigate functional mitochondrial respiration, within integrated mitochondrial networks of fresh brain tissue, to focus on pathologic metabolic pathways following TBI. .

## Materials and Methods

This study was carried out in strict accordance with the recommendations in the Guide for the Care and Use of Laboratory Animals of the National Institutes of Health, and was approved by the Institutional Animal Care and Use Committee of the University of Pennsylvania (Number: 803401). Four-week old (8–10 kg) piglets, with comparable neurodevelopment to a human toddler, were studied (Armstead, 2005; Duhaime, 2006). In an effort to limit heterogeneity, only females were used based on our prior work (Missios et al., 2009). Twenty-eight piglets were randomly assigned to sham or injury cohorts, consisting of a single rapid non-impact rotational injury in the sagittal plane (n=18 injured-RNR, n=10 naïve sham-RNR). Animals were sacrificed 24 hours after TBI.

### Animal Preparation

Anesthetic regimen included: 1) Premedication with an intramuscular injection of ketamine (20 mg/kg) and xylazine (2 mg/kg) 2) Induction: 4% inhaled isoflurane in 1.0 fraction of inspired oxygen via snout mask, until abolishment of response to a reflexive pinch stimulus 3) Maintenance: 1% inhaled isoflurane via endotracheal tube with fraction of inspired oxygen to 0.21. Buprenorphine (0.02 mg/kg) was also delivered intramuscularly for analgesia prior to injury. Circulating water blanket, monitored via a rectal probe, maintained, core body temperature kept constant between 36 and 38C and. Non-invasive blood pressure, oxygen saturation, heart rate, respiratory rate, and end-tidal $CO_2$ were continuously monitored throughout the experiment (Surgivet Advisor V9204; Smith Medical, Waukesha, WI).

### Rapid Non-impact Rotational (RNR) Injury

Diffuse closed head TBI was induced using an established rapid head rotation technique described previously (Eucker et al., 2011; Ibrahim et al., 2010; Raghupathi et al., 2004). While maintained on isoflurane, the head of the piglet was secured to a bite plate by a snout

strap. Isoflurane was withdrawn immediately prior to injury, and the head was rotated rapidly (10–15 ms) ventral-to-dorsal in the sagittal plane with the center of rotation at the cervical spine. The peak angular velocity was nearly constant across the injured group, averaging 126 ± 0.72 radians/second.

Immediately after the RNR, the animal was removed from the injury device. At this angular velocity, rotation direction, and age; animals experienced a brief period of hypoactivity, irritability and gait instability. However, animals do not experience apnea or hemodynamic instability.

Following RNR, animals had significant neurologic deficits, including lethargy and longer periods of recumbancy, and unsteady gait compared to shams. However, animals eventually were able to vocalize, ambulate, maintain body temperature and exhibited proper feeding and drinking behaviors. These injuries are best described as mild-to-moderate in severity, based on parallels with human clinical severity classifications (Adelson et al., 2012; Miller et al., 2012) and neuropathology findings 6 days after RNR (Weeks et al., 2014).

## Preparation of Tissue Homogenates

At 24 hours post-RNR, a craniotomy was performed and a 2 $cm^2$ region of left frontal cortex was resected and both hippocampal regions extracted rapidly (less than 10 seconds) and combined. As a starting point for our initial large animal studies we have chosen 24 hours as our terminal time-point for two critical reasons: 1) We have documented significant injury with neuropathology, imaging and behavior at this time point in our model of diffuse TBI (Jaber et al., 2015; Kilbaugh et al., 2011; 2015; Weeks et al., 2014) 2) other investigators have documented bioenergetic and mitochondrial alterations in rodents following diffuse TBI at this particular time point. The hippocampus and cortex were studied as the areas of interest for two critical factors: 1) Previous studies form our laboratory have documented significant neuropathology and mitochondrial dysfunction within these regions following RNR (Coats and Margulies, 2006; Eucker et al., 2011; Kilbaugh et al., 2011; Weeks et al., 2014) 2) If our hypothesis was consistent with previous findings in adults and infants, and these areas of interest do exhibit alterations in mitochondrial functional pathways; then, these findings would be instrumental in the evaluation of neurobehavioral outcomes in future studies, linking mitochondrial bioenergetics and long-term outcomes (S. Sullivan et al., 2013).

Following extraction, tissue was placed immediately in ice-cold isolation buffer (320 mM sucrose, 10 mM Trizma base, and 2 mM EGTA). Blood and vasculature was dissected and 1 mg of wet weight tissue was gently homogenized on ice in (MiR05 buffer: 110 mM sucrose, 0.5 mM EGTA, 3.0 mM $MgCl_2$, 60 mM K-lactobionate, 10 mM $KH_2PO_4$, 20 mM taurine, 20 mM HEPES and 1.0 g/l fatty acid-free BSA) using a 5 ml Potter-Elvehjem teflon-glass homogenizer to a concentration of 1 mg wet weight tissue/10 μl MiR05 buffer.

## Mitochondrial High-Resolution Respirometry (HRR)

High-resolution Oxygraph-2k (Oroboros Instruments, Innsbruck, Austria) was used to measure mitochondrial respiration. The instrument was calibrated daily, as previously described, and respiration measurements were obtained at a constant 37°C with the addition

of tissue homogenates to a final concentration of 1 mg per ml of Mir05 buffer (Kilbaugh et al., 2015). Oxygen consumption and oxygen flux recorded using Datlab software (5.1, Oroboros Instruments, Innsbruck, Austria)

A substrate, uncoupler, inhibitor titration (SUIT) protocol previously used was specifically designed for porcine brain tissue (Kilbaugh et al., 2015). Complex specific substrates and inhibitors allowed for the assessment of respiratory capacities of the integrated electron transport system (ETS) (Figure 1). Complex I (CI), and complex II (CII) respiratory capacities in brain tissue were evaluated separately; as well as with pathways of convergent electron input through the Q-junction (CI + II) using succinate and nicotinamide adenine dinucleotide (NADH)-linked substrates (Gnaiger, 2009). An optimized dose of digitonin, 1 μl (50 mg/ml), necessary to achieve accurate and consistent oxidative phosphorylation capacity within synaptasomes using water-soluble substrates, and is necessary to achieve similar results in brain tissue homogenates and isolated brain mitochondria (Kilbaugh et al., 2015; 2011). Exogenously administered cytochrome c did not induce a significant effect on mitochondrial respiration at the optimal digitonin dose, indicating an intact outer mitochondrial membrane (data not shown) (Brustovetsky et al., 2002; Sims and Blass, 1986). Sequential additions included: malate (5 mM) and pyruvate (5 mM), followed by ADP (1 mM) and glutamate (5 mM), measuring oxidative phosphorylation capacity of complex I ($OXPHOS_{CI}$), driven by the NADH-related substrates. Succinate (10 mM) was added to stimulate maximal phosphorylating respiration capacity via convergent input through complexes I and II ($OXPHOS_{CI+CII}$). Oligomycin, an ATP-synthase inhibitor, stopped oxidative phosphorylation, inducing LEAK respiration ($LEAK_{CI+CII}$) or State $4_O$ respiration. Maximal convergent non-phosphorylating respiration of the electron transport system ($ETS_{CI+CII}$) was evaluated by titrating the protonophore, carbonyl cyanide p-(trifluoromethoxy) phenylhydrazone (FCCP), until no further increase in respiration was detected. ETS capacity supported by succinate was measured by adding a complex I inhibitor, Rotenone, to reveal complex II-driven respiration ($ETS_{CII}$). ETS electron flow was inhibited by the complex III inhibitor antimycin-A (1 μg/ml), to measure the residual oxygen consumption. This residual value was subtracted from each of the measured respiratory states in the final analysis. Finally, an addition of ascorbate (ASC, 0.8 mM) and N,N,N′,N′-tetramethyl-p-phenylenediamine (TMPD, 0.5 mM), an electron donor to complex IV, measured the activity of cytochrome c oxidase. Complex IV-inhibitor sodium azide (10 mM) was added and the remaining chemical background was subtracted to assess complex IV activity, due to the high level of auto-oxidation of TMPD. The protocol was identical in timing and sequence amongst all groups, sham and injured.

## Citrate Synthase Measurements

Following the completion of respirometry measurements, chamber contents were stored and subsequently analyzed for citrate synthase (CS) activity (μmol/mL/min) quantification (Citrate Synthase Assay Kit, CS0720, Sigma). CS was used as a marker of brain metabolism secondary to its location within the mitochondrial matrix and importance as the first step of the tricarboxylic acid cycle (TCA). In addition, some investigators use CS as a surrogate measure of mitochondrial content per mg of tissue (Bowling et al., 1993; Larsen et al., 2012).

### Data Analysis

Oxygen flux traces were measured automatically with a customized Matlab (Mathworks, Natick, MA) (Kilbaugh et al., 2015). Statistical evaluation was performed using JMP Pro (SAS Institute Inc., version 10.0, Cary, NC, USA). We compared tissue mitochondrial respiration between injured and sham subjects with an unpaired, non-parametric Wilcoxon ranked sum test with Dunn's multiple comparison tests. In addition, paired Wilcoxon ranked sum tests were used to compare regions within sham and injury groups. Differences were considered significant where $p<0.05$. All results are reported as mean ± standard error of the mean (SEM).

## Results

### Mitochondrial Content

We measured CS activity per mg of tissue; there were no differences between brain regions in sham animals (with cortical tissue 24.7 ± 4.5 μmol/mL/min and hippocampal 25.3 ± 6.7 μmol/mL/min, p=0.93) (Figure 2). Diffuse RNR did not stimulate a significant decrease in mitochondrial content following injury in either region (cortex 17.8 ± 0.4 μmol/mL/min, and hippocampus 16.8 ± 0.4 μmol/mL/min) compared to sham animals (cortex 24.7 ± 4.5 μmol/mL/min, p=0.1 and hippocampus 25.3 ± 6.7 μmol/mL/min, p=0.8) (Figure 2). All measures of respiratory capacity within the mitochondrial ETS for each animal were normalized to mitochondrial content by CS activity.

### Rapid Non-impact Rotational (RNR) Injury

We utilized a large animal model of diffuse TBI and evaluated mitochondrial respiration in two regions of interest following RNR injury: cortex and hippocampus (Table 1). In sham animals, mitochondrial respiration, by all measures, were consistently higher in the hippocampus compared to the cortex, and reached significance for $ETS_{CII}$ ($p<0.04$) and $ETS_{CI+CII}$ ($p<0.04$) respiration when values were normalized for mitochondrial content. Post-RNR, all measures of ETS respiration were significantly higher ($p<0.001$) in the hippocampal region compared to cortical respiration ($OXPHOS_{CI}$, $ETS_{CII}$, $OXPHOS_{CI+CII}$, $ETS_{CI+CII}$, $LEAK_{CI+CII}$, and complex IV) following normalization for mitochondrial content (Figure 3).

We then compared each measure per CS and per mg of tissue in sham and RNR injured animals, region by region. Complex I-linked respiration ($OXPHOS_{CI}$) did not differ between RNR and sham animals in the hippocampus (p=0.4) or cortex (p=0.6) when normalized by CS activity (Figure 3); however, $OXPHOS_{CI}$ expressed per mg of tissue was significantly decreased ($p<0.05$) in the cortex compared to sham. Complex II-linked respiration ($ETS_{CII}$) per CS was significantly increased by nearly 20% in the cortex ($p<0.05$) and hippocampus (p=0.02) post-RNR, compared to shams. Furthermore, unlike complex I-driven respiration in the cortex, complex II-driven respiration normalized by tissue weight was not significantly reduced following RNR in either region. Maximal phosphorylating respiration ($OXPHOS_{CI+CII}$) per CS was significantly increased in the hippocampus post-RNR compared to $OXPHOS_{CI+CII}$ in shams, ($p<0.05$), but was not altered in the cortex by RNR injury (p=0.3) (Figure 3A). Maximal uncoupled non-phosphorylating respiration

($ETS_{CI+CII}$) per CS post-RNR did not change from shams in either the hippocampus (p=0.3) or cortex (p=0.6) (Figure 3B). Both $OXPHOS_{CI+CII}$ and $ETS_{CI+CII}$ were significantly reduced (p<0.02) per mg of tissue in the cortex post-RNR compared to sham. Following diffuse TBI, complex IV respiration per CS measured from the hippocampus (p=0.4) and cortex (p=0.7) was similar to complex IV respiration from corresponding regions in shams (Figure 3B). LEAK ($LEAK_{CI+CII}$), or State $4_o$ respiration, was significantly increased post-RNR in hippocampal tissue when normalized by CS activity (p<0.03) (Figure 3B), and per mg of tissue (p<0.01) compared to shams. Cortical tissue post-RNR also exhibited a significant increase in LEAK respiration per CS (p<0.02) compared to shams; and per mg of tissue (p<0.05) compared to shams.

Respiratory ratios were calculated for sham and RNR animals (Table 2). The control ratio for $OXPHOS_{CI+CII}$ ($OXPHOS_{CI+CII}$/LEAK) decreased significantly post-RNR compared to shams in the cortex (p<0.01) and hippocampus (p<0.05) (Table 2). $ETS_{CI+CII}$ control ratio ($ETS_{CI+CII}$/LEAK) also decreased significantly post-RNR, compared to sham animals (Cortex: p<0.006; Hippocampus: p<0.01). The complex I contribution to convergent respiration post-RNR ($ETS_{CI}/ETS_{CI+CII}$) was significantly decreased in the hippocampus compared to sham (p<0.05), and nearly significantly decreased in the cortex following RNR compared to shams (p=0.08) (Table 2). Consequently, the complex II contribution to convergent respiration ($ETS_{CII}/ETS_{CI+CII}$) was significantly greater in the hippocampus post-RNR compared to sham animals (p<0.05), and the increase in the cortex post-RNR nearly reached significance compared to sham (p=0.06).

## Discussion

We report differences in mitochondrial respiration between the cortex and hippocampus in the uninjured immature brain. Our data differs from the uninjured mature rodents where there were no reported differences in basal mitochondria respiration in samples isolated from the striatum, cortex and hippocampus (Sauerbeck et al., 2011). Twenty-four hours after a diffuse traumatic injury to the immature brain, interesting mitochondrial bioenergetic responses emerged, with diffuse injury inducing a significant uncoupling of oxidative and non-oxidative phosphorylation in both the cortex and hippocampus. LEAK respiration, State $4_o$, was significantly increased in both the injured cortical and hippocampal tissues compared to their corresponding regions in sham animals. This increase in LEAK respiration (State $4_o$) in both regions is the predominant factor that influences a significant decrease in RCRs ($OXPHOS_{CI+CII}$ (State 3)/LEAK (State $4_0$)), especially in the hippocampus where $OXPHOS_{CI+CII}$ is significantly increased compared to hippocampal respiration in shams. Our assessments of functional mitochondrial bioenergetics, 24 hours after diffuse TBI, differs from our previously published data in focal injury at the same time-point (Kilbaugh et al., 2015). While there seems to be a common dependence on complex II-driven respiration following both focal and diffuse TBI, diffuse TBI displayed significant uncoupling of oxidative phosphorylation which was not seen in injured tissue following focal TBI (Kilbaugh et al., 2015). The differences in mitochondrial response following diffuse and focal TBI, at similar time-points, emphasizes the heterogeneity of brain injury pathology. Thus, investigations of mitochondrial metabolic pathways following differing injury mechanisms are essential to direct future mitochondrial intervention trials in TBI.

Control ratios $ETS_{CI}/ETS_{CI+CII}$ and $ETS_{CII}/ETS_{CI+II}$ further support the notion that complex I respiration is impaired to some degree following injury, especially in the hippocampus, while convergent respiration via complex II respiration is stimulated at 24 hours post-RNR. This potential compensatory response in convergent respiration may stimulate a significant increase in maximal phosphorylating respiration and a trend toward increased maximal non-phosphorylating respiration in the hippocampus compared to hippocampal mitochondrial respiration in shams. The relative increase in complex II-driven respiration in the cortex and hippocampus when normalized for mitochondrial content may be a compensatory response at 24 hours in an attempt to increase mitochondrial bioenergetic output. We also speculate that the increase in regional hippocampal maximal phosphorylating mitochondrial respiration ($OXPHOS_{CI+CII}$) may be related to increased excitability of hippocampal tissue secondary to pathologic changes in inhibitory function following TBI, triggering increased bioenergetic need to compensate for ongoing secondary injury (Witgen et al., 2005). Yoshino and colleagues presented evidence in rats that hypermetabolism occurred post injury in both the cortex and hippocampus, with an especially marked response in the hippocampus (84.4–91% higher than control) compared to the cortex (30.1–46.6%); however, this hypermetabolic phase only lasted 6 hours before the rodents transitioned to a hypometabolic phase lasting as long as 5 days (Yoshino et al., 1991). With limited research available, the time course and mechanistic response to a purely diffuse injury remains unclear. Future research will need to be conducted to establish correlations between alterations in mitochondrial bioenergetics and outcomes in diffuse immature brain injury.

In addition, an increase in LEAK respiration may represent mitochondrial membrane permeability transition (mPT) and a loss of functional integrity with a dissipation of the proton motive force, or a “protective” uncoupling that limits ATP production to inhibit secondary injury. State $4_o$ or LEAK respiration is determined mainly by proton leak across the inner membrane mediated by endogenous uncoupling proteins (UCPs), which utilize free fatty acids energy potential to translocate protons. When LEAK respiration increases, there is a resultant reduction in the mitochondrial membrane potential ($\Delta\psi$) and ATP production; however, despite the loss of ATP production transient or mild uncoupling may confer neuroprotective properties by limiting ROS generation, mitochondrial $Ca^{2+}$ uptake, and limiting excitotoxic neuronal death (Brand, 2000; Brookes, 2005; Mattiasson et al., 2003; Perez-Pinzon et al., 2012; P. G. Sullivan et al., 2004). This may involve the release of free fatty acids (FFA) that stimulate UCPs, especially UCP2, as a protective anti-ROS mechanism; and, future study will elucidate the mechanism and time courses involved in the immature brain. The timing and mechanism is extremely important, because this uncoupling may limit the ability of mitochondria to increase oxidative phosphorylation in response to ongoing and persistent bioenergetic needs following TBI. Future studies will be performed to delineate the exact molecular cascades and injury timelines in response to diffuse injury.

In our previous study of 3–5-day-old infant piglets we showed that 24 hours, after RNR, there was a significant reduction in maximal phosphorylating respiration (State 3) and a trend towards increases in State $4_0$ respiration compared to sham respiration in both the hippocampus and the cortex, lowering the overall respiratory control ratio (Kilbaugh et al., 2011). To compare the injury severity between these studies, the total injury volume was

measured by β-APP reactivity and hematoxylin and eosin stain via histopathology in a group of N=10 4-week-old piglets with the same RNR in the sagittal direction as the current study, which resulted in an average total injured volume of 0.79 ± 0.08%. In our previous study with 3–5-day-old piglets (n=5), also with a sagittal RNR injury, there was a significantly higher average injured volume of 2.18 ± 0.02%. Based on these findings we postulate that a greater severity of injury post-RNR stimulates a greater reduction in mitochondrial respiration. This postulate correlates with previous work in mature rodents that shows TBI results in the disruption of brain bioenergetics and the resultant bioenergetic deficits are proportional to the degree of severity (Marklund et al., 2006). In more severe brain injury, levels of ATP and other indicators of mitochondrial bioenergetics are significantly reduced at 24 hours and remain depressed for days or weeks (Tavazzi et al., 2005). Conversely, animals with mild TBI (mTBI) had the lowest value of ATP levels at 6 hours with a gradual resolution near sham levels by 24 hours that showed no statistical difference by 5 days post-injury with control animals (Signoretti et al., 2001). A limitation of drawing a direct comparison from our study to studies that quantified ATP levels, is that respirometry provides a functional surrogate marker of ATP synthesis by measuring maximal coupled and uncoupled respiration. The difference between our current study and the previous post-RNR study may be due to developmental differences between infant and toddler, differences in methodology with isolated mitochondrial and tissue homogenates, or the possibility that it may be secondary to injury severity and its effects on mitochondrial function. Further study is critical to understand age-related alterations in mitochondrial bioenergetics, time course of mitochondrial dysfunction, and the effect of injury severity on both age and time course.

### Limitations

Our pilot study of functional, integrated mitochondrial bioenergetic pathways following diffuse TBI generates questions about the complex mechanisms of secondary brain injury following diffuse TBI. Future studies will expand our molecular investigations, including isolated mitochondria and spectrophotometric analysis, to further interrogate the electron transport complex and develop a more complete understanding of the adaptive response and ongoing secondary injury. Finally, in our current experiment there is some variability in our CS measurement in the sham animals which we have not found in our previous studies (Kilbaugh et al., 2015). This was a large animal study with smaller group sizes, and although a small number of animals fell outside of the standard deviation we did not feel it was appropriate from a rigorous scientific/statistical standpoint to exclude these animals from the sham cohort. We presented the data in multiple ways, including data measures independent of the CS, and drew our conclusions based off of all measures of the data.

## Conclusion

We conclude that there are significant alterations in mitochondrial respiration 24 hours after diffuse TBI that varies by location within the brain. In addition, our data suggests that significant uncoupling of oxidative phosphorylation and alterations in convergent respiration through complex I- and complex II-driven respiration. Thus, the results of our immature translational large animal model suggest therapeutic benefit for strategies that support oxidative phosphorylation and bioenergetic output in the developing brain after TBI.

## Acknowledgments

The authors would like to thank Melissa Byro, Ashley Bebee, Jill Ralston, Sarah Sullivan, Albana Shahini, and Saori Morota for their invaluable technical support. The Oroboros Oxygraph used in the study was a loan from NeuroVive Pharmaceutical AB, Lund Sweden. Studies were supported by the NIH UO1 NS069545.

## Reference List

Adelson PD, Pineda J, Bell MJ, Abend NS, Berger RP, Giza CC, Hotz G, Wainwright MS. Pediatric TBI Demographics and Clinical Assessment Working Group. 2012Common data elements for pediatric traumatic brain injury: recommendations from the working group on demographics and clinical assessment. Journal of Neurotrauma. 10.1089/neu.2011.1952

Armstead WM. Age and cerebral circulation. Pathophysiology. 2005; 12:5–15.10.1016/j.pathophys.2005.01.002 [PubMed: 15927820]

Balan IS, Saladino AJ, Aarabi B, Castellani RJ, Wade C, Stein DM, Eisenberg HM, Chen HH, Fiskum G. Cellular Alterations in Human Traumatic Brain Injury: Changes in Mitochondrial Morphology Reflect Regional Levels of Injury Severity. Journal of Neurotrauma. 2013; 30:367–381.10.1089/neu.2012.2339 [PubMed: 23131111]

Bates TE, Almeida A, Heales SJ, Clark JB. Postnatal development of the complexes of the electron transport chain in isolated rat brain mitochondria. Dev Neurosci. 1994; 16:321–327. [PubMed: 7768212]

Bowling AC, Mutisya EM, Walker LC, Price DL, Cork LC, Beal MF. Age-dependent impairment of mitochondrial function in primate brain. Journal of Neurochemistry. 1993; 60:1964–1967. [PubMed: 8473911]

Brand MD. Uncoupling to survive? The role of mitochondrial inefficiency in ageing. Exp Gerontol. 2000; 35:811–820. [PubMed: 11053672]

Brookes PS. Mitochondrial H(+) leak and ROS generation: an odd couple. Free Radic Biol Med. 2005; 38:12–23.10.1016/j.freeradbiomed.2004.10.016 [PubMed: 15589367]

Brustovetsky N, Jemmerson R, Dubinsky JM. Calcium-induced Cytochrome c release from rat brain mitochondria is altered by digitonin. Neurosci Lett. 2002; 332:91–94. [PubMed: 12384218]

Coats B, Margulies SS. Material properties of porcine parietal cortex. J Biomech. 2006; 39:2521–2525.10.1016/j.jbiomech.2005.07.020 [PubMed: 16153652]

Coronado VG, Xu L, Basavaraju SV, McGuire LC, Wald MM, Faul MD, Guzman BR, Hemphill JD. Centers for Disease Control and Prevention (CDC). Surveillance for traumatic brain injury-related deaths--United States, 1997–2007. MMWR Surveill Summ. 2011; 60:1–32. [PubMed: 21544045]

Del Maestro R, McDonald W. Distribution of superoxide dismutase, glutathione peroxidase and catalase in developing rat brain. Mech Ageing Dev. 1987; 41:29–38. [PubMed: 3431167]

Duhaime AC. Large animal models of traumatic injury to the immature brain. Dev Neurosci. 2006; 28:380–387.10.1159/000094164 [PubMed: 16943661]

Duhaime AC, Margulies SS, Durham SR, O'Rourke MM, Golden JA, Marwaha S, Raghupathi R. Maturation-dependent response of the piglet brain to scaled cortical impact. Journal of Neurosurgery. 2000; 93:455–462.10.3171/jns.2000.93.3.0455 [PubMed: 10969944]

Durham SR, Duhaime AC. Basic science; maturation-dependent response of the immature brain to experimental subdural hematoma. Journal of Neurotrauma. 2007; 24:5–14.10.1089/neu.2006.0054 [PubMed: 17263666]

Eucker SA, Smith C, Ralston J, Friess SH, Margulies SS. Physiological and histopathological responses following closed rotational head injury depend on direction of head motion. Experimental Neurology. 2011; 227:79–88.10.1016/j.expneurol.2010.09.015 [PubMed: 20875409]

Gean AD, Fischbein NJ. Head trauma. Neuroimaging Clin N Am. 2010; 20:527–556.10.1016/j.nic.2010.08.001 [PubMed: 20974375]

Gilmer LK, Ansari MA, Roberts KN, Scheff SW. Age-related mitochondrial changes after traumatic brain injury. Journal of Neurotrauma. 2010; 27:939–950.10.1089/neu.2009.1181 [PubMed: 20175672]

Glenn TC, Kelly DF, Boscardin WJ, Mcarthur DL, Vespa PM, Oertel M, Hovda DA, Bergsneider M, Hillered L, Martin NA. Energy dysfunction as a predictor of outcome after moderate or severe head injury: indices of oxygen, glucose, and lactate metabolism. J Cereb Blood Flow Metab. 2003; 23:1239–1250.10.1097/01.WCB.0000089833.23606.7F [PubMed: 14526234]

Gnaiger E. Capacity of oxidative phosphorylation in human skeletal muscle: new perspectives of mitochondrial physiology. Int J Biochem Cell Biol. 2009; 41:1837–1845.10.1016/j.biocel.2009.03.013 [PubMed: 19467914]

Grate LL, Golden JA, Hoopes PJ, Hunter JV, Duhaime AC. Traumatic brain injury in piglets of different ages: techniques for lesion analysis using histology and magnetic resonance imaging. Journal of Neuroscience Methods. 2003; 123:201–206. [PubMed: 12606068]

Ibrahim NG, Ralston J, Smith C, Margulies SS. Physiological and pathological responses to head rotations in toddler piglets. Journal of Neurotrauma. 2010; 27:1021–1035.10.1089/neu.2009.1212 [PubMed: 20560753]

Jaber SM, Sullivan S, Margulies SS. Noninvasive metrics for identification of brain injury deficits in piglets. Dev Neuropsychol. 2015; 40:34–39.10.1080/87565641.2014.969733 [PubMed: 25649778]

Kilbaugh TJ, Bhandare S, Lorom DH, Saraswati M, Robertson CL, Margulies SS. Cyclosporin a preserves mitochondrial function after traumatic brain injury in the immature rat and piglet. Journal of Neurotrauma. 2011; 28:763–774.10.1089/neu.2010.1635 [PubMed: 21250918]

Kilbaugh TJ, Karlsson M, Byro M, Bebee A, Ralston J, Sullivan S, Duhaime AC, Hansson MJ, Elmér E, Margulies SS. Mitochondrial bioenergetic alterations after focal traumatic brain injury in the immature brain. Experimental Neurology. 2015; 271:136–144.10.1016/j.expneurol.2015.05.009 [PubMed: 26028309]

Larsen S, Nielsen J, Hansen CN, Nielsen LB, Wibrand F, Stride N, Schroder HD, Boushel R, Helge JW, Dela F, Hey-Mogensen M. Biomarkers of mitochondrial content in skeletal muscle of healthy young human subjects. J Physiol (Lond). 2012; 590:3349–3360.10.1113/jphysiol.2012.230185 [PubMed: 22586215]

Lifshitz J, Friberg H, Neumar RW, Raghupathi R, Welsh FA, Janmey P, Saatman KE, Wieloch T, Grady MS, McIntosh TK. Structural and functional damage sustained by mitochondria after traumatic brain injury in the rat: evidence for differentially sensitive populations in the cortex and hippocampus. J Cereb Blood Flow Metab. 2003; 23:219–231. [PubMed: 12571453]

Lifshitz J, Sullivan PG, Hovda DA, Wieloch T, McIntosh TK. Mitochondrial damage and dysfunction in traumatic brain injury. MITOCHONDRION. 2004; 4:705–713.10.1016/j.mito.2004.07.021 [PubMed: 16120426]

Marcoux J, McArthur DA, Miller C, Glenn TC, Villablanca P, Martin NA, Hovda DA, Alger JR, Vespa PM. Persistent metabolic crisis as measured by elevated cerebral microdialysis lactate-pyruvate ratio predicts chronic frontal lobe brain atrophy after traumatic brain injury. Critical Care Medicine. 2008; 36:2871–2877.10.1097/CCM.0b013e318186a4a0 [PubMed: 18766106]

Marklund N, Salci K, Ronquist G, Hillered L. Energy metabolic changes in the early post-injury period following traumatic brain injury in rats. Neurochem Res. 2006; 31:1085–1093.10.1007/s11064-006-9120-0 [PubMed: 16909313]

Mattiasson G, Shamloo M, Gido G, Mathi K, Tomasevic G, Yi S, Warden CH, Castilho RF, Melcher T, Gonzalez-Zulueta M, Nikolich K, Wieloch T. Uncoupling protein-2 prevents neuronal death and diminishes brain dysfunction after stroke and brain trauma. Nat Med. 2003; 9:1062–1068.10.1038/nm903 [PubMed: 12858170]

Miller AC, Odenkirchen J, Duhaime AC. 2012Common data elements for research on traumatic brain injury: Pediatric considerations. Journal of ….

Missios S, Harris BT, Dodge CP, Simoni MK, Costine BA, Lee YL, Quebada PB, Hillier SC, Adams LB, Duhaime AC. Scaled cortical impact in immature swine: effect of age and gender on lesion volume. Journal of Neurotrauma. 2009; 26:1943–1951.10.1089/neu.2009-0956 [PubMed: 19469691]

Perez-Pinzon MA, Stetler RA, Fiskum G. Novel mitochondrial targets for neuroprotection. Journal of Cerebral Blood Flow & Metabolism. 2012; 32:1362–1376.10.1038/jcbfm.2012.32 [PubMed: 22453628]

Ragan DK, McKinstry R, Benzinger T, Leonard JR, Pineda JA. Alterations in cerebral oxygen metabolism after traumatic brain injury in children. J Cereb Blood Flow Metab. 2013; 33:48–52.10.1038/jcbfm.2012.130 [PubMed: 22968318]

Raghupathi R, Mehr MF, Helfaer MA, Margulies SS. Traumatic axonal injury is exacerbated following repetitive closed head injury in the neonatal pig. Journal of Neurotrauma. 2004; 21:307–316.10.1089/089771504322972095 [PubMed: 15115605]

Robertson CL, Scafidi S, McKenna MC, Fiskum G. Mitochondrial mechanisms of cell death and neuroprotection in pediatric ischemic and traumatic brain injury. Experimental Neurology. 2009; 218:371–380.10.1016/j.expneurol.2009.04.030 [PubMed: 19427308]

Sauerbeck A, Pandya J, Singh I, Bittman K, Readnower R, Bing G, Sullivan P. Analysis of regional brain mitochondrial bioenergetics and susceptibility to mitochondrial inhibition utilizing a microplate based system. Journal of Neuroscience Methods. 2011; 198:36–43.10.1016/j.jneumeth.2011.03.007 [PubMed: 21402103]

Signoretti S, Marmarou A, Tavazzi B, Lazzarino G, Beaumont A, Vagnozzi R. N-Acetylaspartate reduction as a measure of injury severity and mitochondrial dysfunction following diffuse traumatic brain injury. Journal of Neurotrauma. 2001; 18:977–991.10.1089/08977150152693683 [PubMed: 11686498]

Sims NR, Blass JP. Expression of classical mitochondrial respiratory responses in homogenates of rat forebrain. Journal of Neurochemistry. 1986; 47:496–505. [PubMed: 3734792]

Sullivan PG, Springer JE, Hall ED, Scheff SW. Mitochondrial uncoupling as a therapeutic target following neuronal injury. J Bioenerg Biomembr. 2004; 36:353–356.10.1023/B:JOBB.0000041767.30992.19 [PubMed: 15377871]

Sullivan S, Eucker SA, Gabrieli D, Bradfield C, Coats B, Maltese MR, Lee J, Smith C, Margulies SS. White matter tract-oriented deformation predicts traumatic axonal brain injury and reveals rotational direction-specific vulnerabilities. Biomech Model Mechanobiol. 2015; 14:877–896.10.1007/s10237-014-0643-z [PubMed: 25547650]

Sullivan S, Friess SH, Ralston J, Smith C, Propert KJ, Rapp PE, Margulies SS. Improved behavior, motor, and cognition assessments in neonatal piglets. Journal of Neurotrauma. 2013 130613004306008. 10.1089/neu.2013.2913

Tavazzi B, Signoretti S, Lazzarino G, Amorini AM, Delfini R, Cimatti M, Marmarou A, Vagnozzi R. Cerebral oxidative stress and depression of energy metabolism correlate with severity of diffuse brain injury in rats. Neurosurgery. 2005; 56:582–9. discussion 582–9. [PubMed: 15730584]

Weeks D, Sullivan S, Kilbaugh TJ, Smith C, Margulies SS. Influences of developmental age on the resolution of diffuse traumatic intracranial hemorrhage and axonal injury. Journal of Neurotrauma. 2014; 31:206–214.10.1089/neu.2013.3113 [PubMed: 23984914]

Witgen BM, Lifshitz J, Smith ML, Schwarzbach E, Liang SL, Grady MS, Cohen AS. Regional hippocampal alteration associated with cognitive deficit following experimental brain injury: a systems, network and cellular evaluation. Neuroscience. 2005; 133:1–15.10.1016/j.neuroscience.2005.01.052 [PubMed: 15893627]

Xu Y, Mcarthur DL, Alger JR, Etchepare M, Hovda DA, Glenn TC, Huang S, Dinov I, Vespa PM. Early nonischemic oxidative metabolic dysfunction leads to chronic brain atrophy in traumatic brain injury. J Cereb Blood Flow Metab. 2010; 30:883–894.10.1038/jcbfm.2009.263 [PubMed: 20029449]

Yoshino A, Hovda DA, Kawamata T, Katayama Y, Becker DP. Dynamic changes in local cerebral glucose utilization following cerebral conclusion in rats: evidence of a hyper- and subsequent hypometabolic state. Brain Research. 1991; 561:106–119. [PubMed: 1797338]

## Highlights

- Diffuse traumatic brain injury results in significant uncoupling of oxidative phosphorylation.
- Alterations in convergent respiration through complex I- and complex II-driven respiration.
- Complex-II driven respiration increased 24 hours after diffuse traumatic brain injury.
- Heterogeneity of mitochondrial response following differing mechanism of injury and age

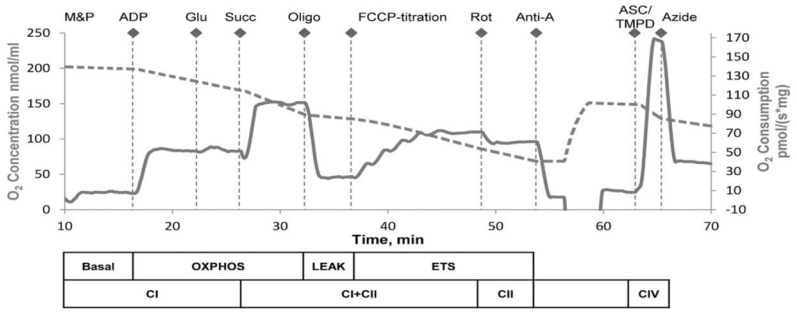


**Figure 1. Oxygen concentration and consumption example trace from SUIT protocol**

The graph depicts an illustrative trace of oxygen consumption rate using a substrate, uncoupler, inhibitor titration (SUIT) protocol. Induced respiratory states and respiratory complexes activated are outlined below the x-axis. After stabilization at basal respiration with endogenous substrates, and in the presence of digitonin, the SUIT protocol was executed as indicated above the oxygen concentration trace. M&P, malate + pyruvate; Glu, glutamate; Succ, succinate; Oligo, oligomycin; Rot, rotenone; Anti-A, antimycin-A; ASC/TMPD, ascorbate and TMPD.

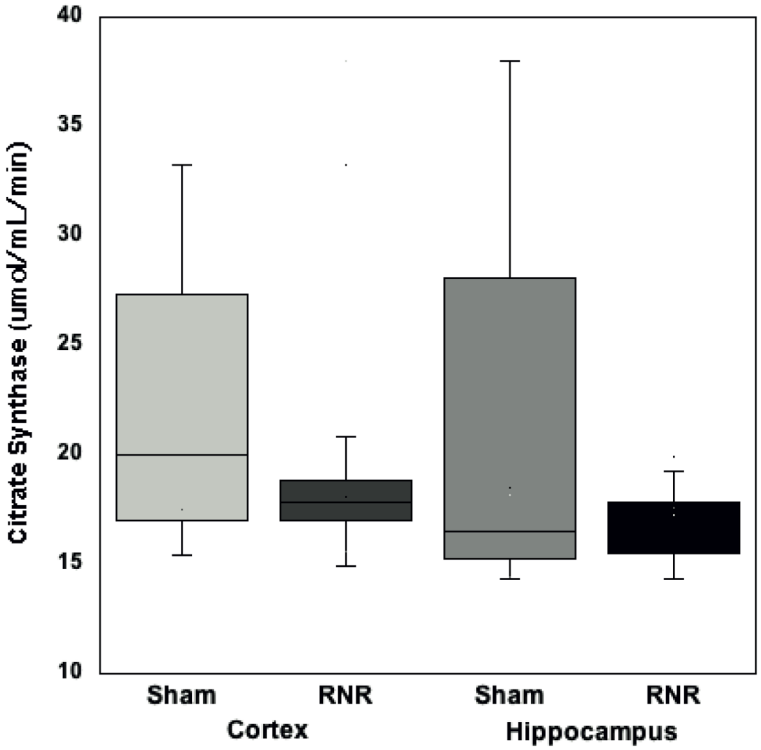


**Figure 2. Citrate synthase activity**

24 hours post-RNR there was a no significant decrease in citrate synthase activity in either region compared to sham animals (p=0.19 hippo and p=0.29 cortex). Boxplots: Horizontal lines represent the median CS activity, with the box representing the 25$^{th}$ and 75$^{th}$ percentiles, the whiskers the 5$^{th}$ and 95$^{th}$ percentiles, and the outliers

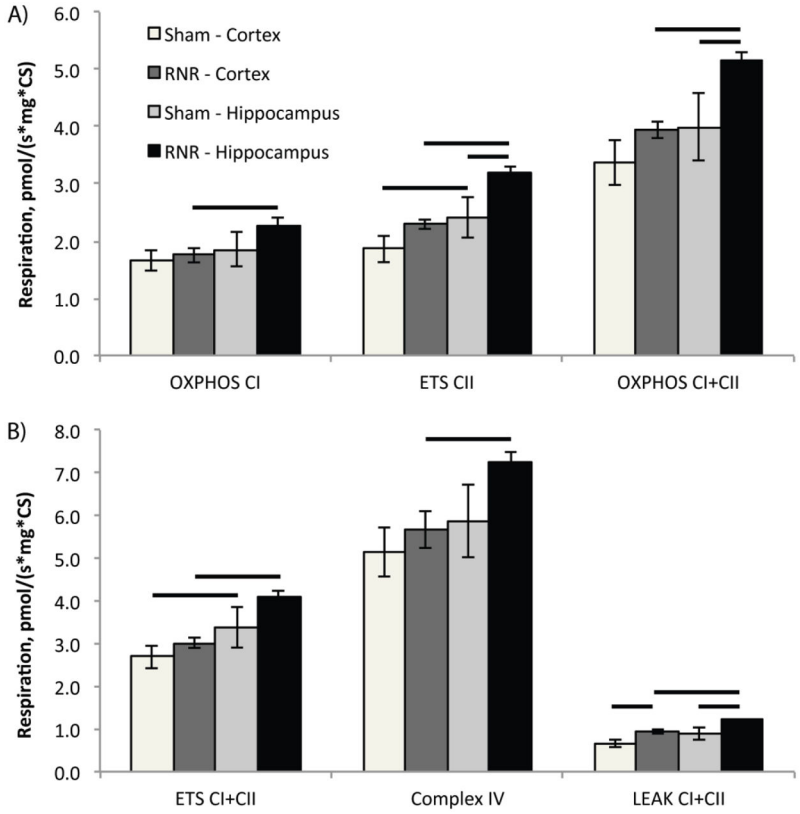


**Figure 3. Mitochondrial respiration from RNR injured and shams normalized by mitochondrial content (citrate synthase) measured 24 hours post TBI**

A) At 24 hours post-RNR Complex II-driven respiration, $ETS_{CII}$ and maximal, coupled phosphorylating respiration $OXPHOS_{CI+CII}$ was significantly increased compared to hippocampal respiration from sham animals. B) In addition, $LEAK_{CI+CII}$ respiration is significantly increased in both injured regions compared to corresponding regions in sham animals. Presented as mean ± SEM. For definitions of respiratory states and substrates utilized please see Figure 1. Bars, $p < 0.05$.

**Table 1**

Respiration of brain tissue homogenates from sham and diffuse rapid non-impact rotational TBI

| Respiratory Parameters | Per mg of tissue (pmols $O_2$/s* mg) | | | | Per CS activity (pmols $O_2$/s* mg* CS) | | | |
|---|---|---|---|---|---|---|---|---|
| | Sham (n=10) | | RNR (n=18) | | Sham (n=10) | | RNR (n=18) | |
| | Cortex | Hippo | Cortex | Hippo | Cortex | Hippo | Cortex | Hippo |
| $OXPHOS_{CI}$ | 38.0±2.7 | 39.6±2.8 | 29.7±1.8* | 35.9±2.8 | 1.6±0.2 | 1.9±0.3 | 1.8±0.1 | 2.3±0.1 |
| $ETS_{CII}$ | 41.6±2.1 | 47.3±3.1 | 36.7±2.4 | 47.8±3.3 | 1.9±0.1 | 2.4±0.4 | 2.3±0.1* | 3.2±0.1* |
| $OXPHOS_{CI+CII}$ | 76.0±4.0 | 80.6±6.0 | 67.7±1.9* | 82.4±3.5 | 3.4±0.4 | 4.0±0.6 | 3.9±0.1 | 5.2±0.2* |
| $ETS_{CI+CII}$ | 61.2±3.1 | 67.6±3.9 | 51.2±1.8* | 66.1±2.3 | 2.7±0.3 | 3.4±0.5 | 3.0±0.1 | 4.1±0.1* |
| Complex IV | 106.4±5.5 | 121.5±8.3 | 98.3±5.9 | 118.5±3.5 | 5.1±0.6 | 5.9±0.9 | 5.7±0.4 | 7.3±0.2* |
| $LEAK_{CI+CII}$ | 13.9±0.9 | 16.3±0.8 | 16.1±0.9* | 19.2±0.6* | 0.67±0.2 | 0.86±0.1 | 0.93±0.2* | 1.2±0.04* |

Mitochondrial respiration of brain tissue homogenates from the Cortex (Cortex) and Hippocampus (Hippo) region in two cohorts: sham and 24 hours post-Rapid Non-impact Rotational Injury (RNR). Respiration is expressed per mg of tissue (pmols O2/s*mg), and per citrate synthase activity (pmols O2/s*CS) to normalize data for mitochondrial content. Presented as mean ± SEM;

* $p < 0.05$ significant different from corresponding sham region.

For definitions of respiratory states and substrates utilized, please see Figure 1.

## Table 2

Respiratory ratios of brain tissue homogenates from sham and diffuse rapid non-impact rotational TBI

| **Respiratory Ratios** | **Sham (n=10)** | | **CCI (n=18)** | |
|---|---|---|---|---|
| | **Cortex** | **Hippo** | **Cortex** | **Hippo** |
| $OXPHOS_{CI+CII}$/LEAK | 5.7±0.4 | 5.0±0.3 | 4.3±0.2* | 4.3±0.2* |
| $ETS_{CI+CII}$/LEAK | 4.6±0.4 | 4.3±0.2 | 3.3±0.2* | 3.4±0.1* |
| $ETS_{CI}/ETS_{CI+CII}$ | 0.32±0.02 | 0.31±0.02 | 0.29±0.04 | 0.28±0.04* |
| $ETS_{CII}/ETS_{CI+CII}$ | 0.68±0.02 | 0.69±0.02 | 0.71±0.01* | 0.72±0.04* |
| $ETS_{CII}/ETS_{CI}$ | 2.32±0.23 | 2.40±0.17 | 3.1±0.34* | 3.33±0.33* |

Respiratory ratios were also calculated. $ETS_{CI}$ was calculated by subtracting $ETS_{CI+CII}$ minus $ETS_{CII}$. Presented as mean ± SEM;

* $p < 0.05$ significant different from corresponding sham region respiratory ratio.

For definitions of respiratory states and substrates utilized, please see Figure 1.